Available online at www.sciencedirect.com
SCIENCE DIRECT
Journal of Catalysis 236 (2005) 45–54
JOURNAL OF CATALYSIS
www.elsevier.com/locate/jcat

Alkylation of toluene with propene over H-MCM-22 zeolite. Location of the main and secondary reactions

J. Rigoreau, S. Laforge, N.S. Gnep, M. Guisnet *

Laboratoire de Catalyse en Chimie Organique, UMR 6503 CNRS - Université de Poitiers, Faculté des Sciences, 40 avenue du Recteur Pineau, 86022 Poitiers cedex, France

Received 7 March 2005; revised 1 September 2005; accepted 6 September 2005

Available online 13 October 2005

Abstract

Alkylation of toluene with propene was carried out at 200 °C over a H-MCM-22 sample (Si/Al = 15) for which the distribution of protonic acid sites in the three pore systems (supercages, sinusoidal channels, and external hemicages) was estimated by various methods. Different reactions were shown to take place in each of the pore systems. The desired alkylation of toluene into cymenes (and diisopropyltoluenes) occurs only within the external hemicages and without any deactivation. C_4–C_6 alkene production through propene oligomerization cracking was demonstrated to occur essentially within the sinusoidal channels. Mainly nondesorbed products (coke) are formed within the supercages.
© 2005 Elsevier Inc. All rights reserved.

Keywords: MCM-22 zeolite; Cymene production; Toluene alkylation; Propene oligomerization; Coking; Location of reactions

1. Introduction

Zeolite MCM-22 (MWW), synthesized by Mobil researchers in 1990 [1], is now used for the liquid phase alkylation of benzene with ethene and propene (Mobil-Raytheon processes [2,3]). The Mobil-Raytheon cumene process produces very pure cumene (99.97 wt%) at 99.7 wt% yield. Commercially, the MCM-22 catalyst has demonstrated cycle lengths >2 years, the ultimate life cycle being likely >5 years. The high selectivity of MCM-22 against propene oligomerization and polyalkylation allows the process to operate at low benzene-to-propene ratios. However, according to Perego and Ingallina [3], the BEA zeolite developed by Enichem would be more suitable than MCM-22 for cumene synthesis, whereas this would be the reverse for ethylbenzene synthesis.

MCM-22 is a very particular zeolite. Indeed, in contrast to most other zeolites, MCM-22 contains independent pore systems: large supercages (18.2 × 7.1 × 7.1 Å) connected by 10-MR openings (4.0 × 5.5 Å), bidimensional sinusoidal channels (4.1 × 5.1 Å), and large external cups, corresponding to hemisupercages (7.0 ×7.1 × 7.1 Å) [4,5]. Because of the very different shapes and sizes of these three pore systems and the varying activity of their acid sites (turnover frequency [TOF]), the selectivity and sensitivity to deactivation of the reactions that occur there would be very different. This was previously shown for *m*-xylene transformation; the value of TOF was 2 and 2.7 times higher for the protonic sites of the external cups than for those located in the supercages and sinusoidal channels, respectively [6]. Furthermore, in the large external cups the main reaction of *m*-xylene is a non-shape-selective isomerization, a *para*-xylene to *ortho*-xylene (p/o) ratio of 1.1. In the sinusoidal channels, only *m*-xylene isomerization into *p*-xylene can occur; *o*-xylene is unable to desorb from or to enter those channels, as has been shown by adsorption experiments [7]. In the supercages, both *m*-xylene isomerization and disproportionation occur. However, because of product shape selectivity effects, the p/o ratio is much greater than 1 (3.5–4), and the bulky trimethylbenzenes trapped within the supercages undergo various transformations, leading to smaller products and to "coke" [8]. Consequently, very fast deactivation of the supercages can be observed. In contrast, there is practically no deactivation of the reactions occurring in the sinusoidal channels and in the external cups. This can be related to the difficulty of forming and trapping "coke" precursors within the sinu-

* Corresponding author. Fax: +33 5 49 45 37 79.
E-mail address: michel.guisnet@univ-poitiers.fr (M. Guisnet).

0021-9517/$ – see front matter © 2005 Elsevier Inc. All rights reserved.
doi:10.1016/j.jcat.2005.09.008

soidal channels (quasi-identical sizes of the channel apertures and channel intersections) and within the large external cups with small depth, from which molecules can be easily desorbed.

The aim of this study is to determine the roles of the three pore systems of a MCM-22 zeolite in the gas phase alkylation of toluene with propene, chosen as a model reaction of cumene synthesis. The essential role of the protonic sites of the external cups in aromatic alkylation [9–12] is confirmed. Moreover, it is shown that oligomerization cracking of propene, which is the main secondary reaction over fresh MCM-22, occurs essentially on the protonic sites of the sinusoidal channels. The deactivation of these reactions is completely different, negligible for alkylation, and very fast for oligomerization cracking.

2. Experimental

2.1. Materials

The MCM-22 laminar precursor, with a Si/Al ratio of 16.8, synthesized as described previously [13], was calcined under dry air flow at 550 °C for 12 h. The protonic form of the material was obtained by two successive exchanges with a 2 M NH_4NO_3 solution for 1 h at 80 °C under reflux, followed by calcination at 500 °C for 3 h.

Sample porosity was characterized by nitrogen adsorption at −196 °C with a Micromeritics Tristar apparatus. Before adsorption, the sample was pretreated at 350 °C under vacuum for 12 h.

2.2. Infrared experiments

Infrared (IR) spectra were recorded on a Nicolet NEXUS FTIR spectrometer. Before measurements, thin (5–15 mg) zeolite wafers were pretreated in situ at 450 °C for 12 h under air flow (1 mL min^{-1}) and then at 200 °C for 1 h under vacuum (10^{-3} Torr).

Pyridine was adsorbed at 150 °C and then evacuated in vacuum (10^{-3} Torr for 1 h), to eliminate the physisorbed pyridine molecules. The concentrations in Brönsted and Lewis acid sites were estimated from the areas of the bands at 1545 and 1450 cm^{-1}, respectively, using extinction coefficients determined previously [14].

Because 2,4-dimethylquinoline (2,4-DMQ) is not sufficiently volatile to allow its introduction in the gas phase, a small amount of 2,4-DMQ was solubilized in methylene chloride (20–40 µmol in 1 mL of solvent) and deposited homogeneously on the pretreated zeolite wafer. Then the solvent was evacuated in vacuum at 120 °C, and IR spectra of adsorbed 2,4-DMQ were recorded. The temperature was then increased to 200 °C without evacuation for 20 min. Evacuation in vacuum was then performed for 3 min, and IR spectra were recorded. The concentration in 2,4-dimethylquinolinium ions was estimated from the area of the band at 1649 cm^{-1} using the extinction coefficient determined previously [15].

2.3. Toluene–propene transformation

The transformation of the toluene–propene mixture was carried out in a fixed-bed reactor under the following conditions: 200 °C, atmospheric pressure, $p_{N_2}/p_{toluene} = 5$ and $p_{toluene}/p_{propene} = 2$, contact time (taken as the reverse of the weight hourly space velocity) of $\tau = 0.0048$–0.0288 h g_{cat} $g_{toluene}^{-1}$. Toluene was percolated on a silica gel column to eliminate traces of peroxide. This reactant was injected in a vaporization spiral at the top of the reactor, in a flow of nitrogen and propene, using a Metrohm Dosimat 725 automatic syringe. Before reaction, the catalyst was activated in situ at 450 °C under dry air flow overnight, then cooled to the reaction temperature under nitrogen flow. The reaction products were collected with a 10-position valve and analyzed on-line by a gas chromatograph (Varian 3400) equipped with a flame ionization detector and a 60 m DB1 (J&W Scientific) capillary column, with H_2 as the carrier gas.

After reaction, the samples were quickly cooled to room temperature under nitrogen flow and kept refrigerated. The coke content of the samples was measured by total burning at 1020 °C under helium and oxygen with a Thermoquest analyzer. The effect of γ-collidine poison on toluene–propene transformation was determined by adding a small amount (25 µL in 10 mL of toluene) of collidine to the reactant.

3. Results and discussion

3.1. Physicochemical characteristics of the MCM-22 zeolite

3.1.1. Pore volume and external surface

Scanning electron microscopy showed that the sample was constituted mainly of platelets with a thickness of approximately 0.05–0.1 µm and a size of 0.5 × 0.5 $µm^2$ agglomerated into particles. The nitrogen adsorption isotherm was analyzed by both the Dubinin–Raduskevich (DR) and t-plot (tp, using the Harkins–Jura equation [16]) methods. The micropore volume (pore diameter < 20 Å), V_{DR}, and V_{tp} (Table 1) represents 40–45% of the total pore volume (estimated at $p/p_0 = 0.97$). The difference between total and micropore volumes (55–60%)

Table 1
Physicochemical characteristics of the MCM-22 sample

Porosity					Acidity (µmol g^{-1})	
V_{total} (cm^3 g^{-1})	V_{DR} (cm^3 g^{-1})	V_{tp} (cm^3 g^{-1})	V_{meso} (cm^3 g^{-1})	S_{EXT} (m^2 g^{-1})	C_B	C_L
0.487	0.227	0.193	0.260	92	550	63

V_{total}, total pore volume; V_{DR}, micropore volume using the Dubinin–Raduskevich equation; V_{tp}, micropore volume using the t-plot method; V_{meso}, mesopore volume; S_{ext}, external surface using the t-plot method; C_B/C_L, concentration of Brönsted/Lewis acid sites estimated by pyridine adsorption/desorption at 150 °C followed by IR spectroscopy.

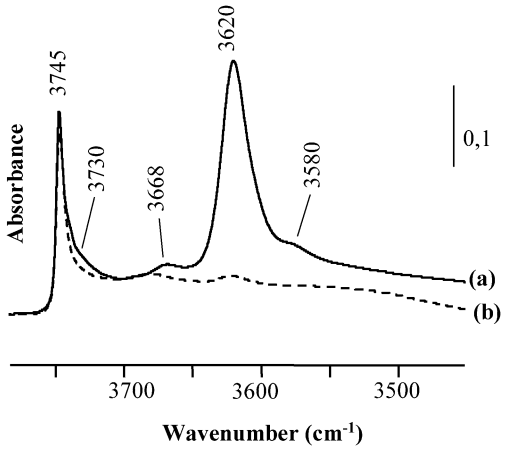

Fig. 1. IR spectra of the MCM-22 sample in the OH stretching region: (a) before pyridine adsorption; (b) after pyridine evacuation at 150 °C.

is mainly due to interparticle mesopores. The external surface estimated by the t-plot method was found to be equal to 92 $m^2\,g^{-1}$.

3.1.2. Total acid site concentration

In agreement with previous works [17,18], four hydroxyl bands appeared in the IR spectrum of the sample (Fig. 1). The main band at 3620 cm^{-1}, with a shoulder at 3580 cm^{-1}, corresponds to bridged hydroxyl groups (Al–OH–Si). A small band at 3668 cm^{-1} can be related to hydroxyl groups linked to extra-framework Al species (EFAL) probably formed during the calcination procedure. Finally, two bands at 3730 and 3745 cm^{-1} can be attributed to internal and external silanols groups, respectively [17].

Adsorption of pyridine followed by evacuation at 150 °C (Fig. 1) shows that the quasitotality of the bridged OH groups interacts with pyridine with <2% of the surface of the corresponding band remaining apparent. The intensities of the bands at 3668 and 3730 cm^{-1} were also affected, but the band at 3745 cm^{-1} (external silanols groups) was not. The concentrations of Brönsted and Lewis acid sites, C_B and C_L, were estimated from the intensities of the bands at 1545 and 1450 cm^{-1} corresponding to pyridinium ions (Py–H^+) and to pyridine coordinated to Lewis sites (Py–L), respectively, using the extinction coefficients determined previously [14]. The values obtained after pyridine desorption at 150 °C are reported in Table 1.

3.1.3. Concentration of protonic sites in the external cups

The concentration of protonic sites in the external hemicages was first determined by 2,4-DMQ adsorption followed by IR spectroscopy [15]. Indeed, this molecule is too bulky to diffuse through the narrow apertures of supercages and of sinusoidal channels, and hence can be protonated only on the protonic sites of the external cups. Therefore, the concentration of these latter sites can be considered as equivalent to that of the 2,4-dimethylquinolinium ions (80–100 µmol g^{-1} in our sample). This concentration can also be estimated through poisoning experiments with 2,4-DMQ during m-xylene transformation at

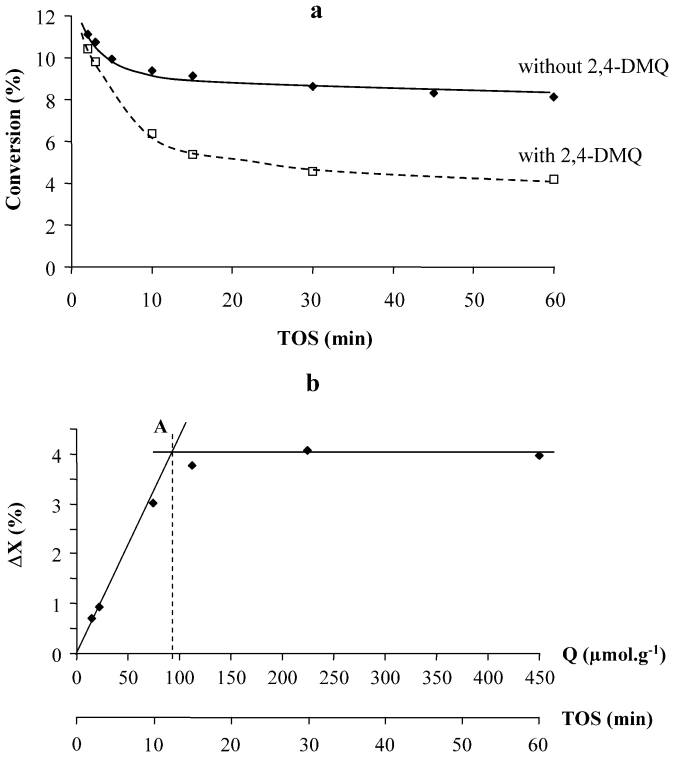

Fig. 2. Transformation of m-xylene on MCM-22 as a function of time-on-stream (TOS) in presence and absence of 2,4-DMQ (a), and decrease in m-xylene conversion (ΔX) as a function of the amount of 2,4-DMQ (Q) (b).

350 °C [6]. The procedure for this, originally developed to estimate the concentration of the external active sites (which are protonic sites), was applied to our HMCM-22 sample (Fig. 2). The effect of time-on-stream (TOS) was compared for the transformation of m-xylene pure and added with 2,4-DMQ. In both cases, an initial decrease in conversion followed by a quasi-plateau for TOS > 20 min can be observed; of course, the decrease was more significant in the presence of the 2,4-DMQ poison (Fig. 2a). The difference between m-xylene conversion in the absence and in presence of 2,4-DMQ (ΔX), which corresponds to the poisoning effect of 2,4-DMQ, was plotted as a function of TOS and of the amount of 2,4-DMQ that passed on the zeolite (Fig. 2b). The maximum value of ΔX (4.1%) corresponded to the conversion of m-xylene on the protonic sites of the external cups. Comparing this value with the conversion of m-xylene over fresh HMCM-22 (11.1%) shows that 37% of the activity of the HMCM-22 originated from the protonic sites of the external cups. Moreover, by admitting that at short TOS values, all of the 2,4-DMQ molecules passing on the zeolite have a poisoning effect, the amount of 2,4-DMQ needed for complete deactivation of the external sites (and hence the concentration of these sites) will be given by the Q value of point A (Fig. 2b). The value obtained (90 µmol g^{-1}; 16% of the total sites) was very close to that estimated by 2,4-DMQ adsorption followed by IR spectroscopy (80–100 µmol g^{-1}). Thus these sites are more active than the internal sites: 37% of the m-xylene transformation for 16% of the sites (only), owing to diffusion control of the reaction within the inner micropores.

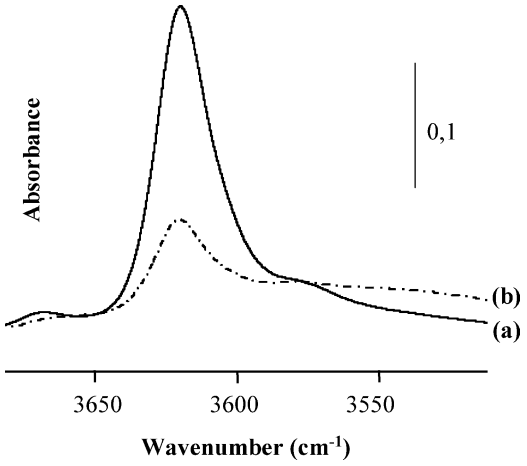

Fig. 3. IR spectra of the MCM-22 sample in the OH stretching region: (a) fresh sample; (b) after transformation of *m*-xylene for 24 h.

3.1.4. Concentration of protonic sites in the supercages and in sinusoidal channels

The concentration of the protonic sites in the inner micropores can be estimated simply by the difference between the total concentration of protonic sites in the zeolite measured by adsorption of pyridine at 150 °C (Table 1) and the concentration of these sites within the external cups. Approximately 460 μmol g^{-1} will be located within the inner micropores.

The difference spectra (before minus after pyridine adsorption) obtained for a desorption temperature of 150 °C can be used to specify the distribution of the bridged hydroxyl groups in the three locations proposed by Onida et al. [19]. The following values, similar to those found with other MCM-22 samples [17], were obtained: ∼60% in the supercages, 22–24% in the sinusoidal channels, and 16–18% linked to the framework of the hexagonal prisms between two supercages. Therefore, approximately 280 μmol g^{-1} of protonic sites would be located within the supercages, 105 μmol g^{-1} within the sinusoidal channels, and 75 μmol g^{-1} linked to the framework of the hexagonal prisms between two supercages. These latter sites may be accessible from both supercages and sinusoidal channels [17].

The concentration of protonic sites of the supercages or accessible through these supercages can be estimated by comparing the intensities of the bridged OH band at 3620 cm^{-1} before and after *m*-xylene transformation for 24 h (Fig. 3), that is, after complete deactivation of the supercage sites [6]. A significant decrease of the band (∼75%) can be observed, corresponding to the interaction of the supercage protonic sites with the coke molecules. This means that ∼75% of the inner sites (i.e., 345 μmol $g^{-1}_{zeolite}$) would be located or accessible via the supercages, with the other sites (i.e., 115 μmol $g^{-1}_{zeolite}$) located or accessible via the sinusoidal channels. Comparing these values with those obtained by deconvolution suggests that most protonic sites of the hexagonal prisms between two supercages are likely accessible through the supercages.

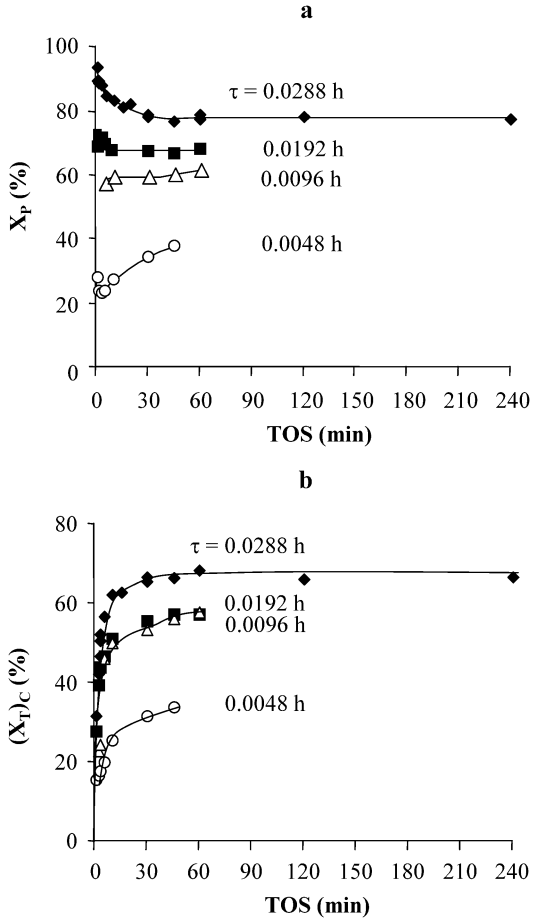

Fig. 4. Transformation of a 2/1 toluene–propene mixture at 200 °C over a MCM-22 zeolite. Effect of time-on-stream (TOS) on propene conversion X_P (a) and toluene conversion $(X_T)_C$ (b) for several contact times τ.

3.2. Transformation of the propene–toluene mixture: reaction scheme

The transformation of the 1/2 molar mixture of propene and toluene was carried out at four different contact times of toluene, τ (taken as the reverse of the weight hourly space velocity): 0.0048, 0.0096, 0.0192, and 0.0288 h $g_{zeolite}$ $g^{-1}_{toluene}$. For the higher values of τ, there was a decrease with TOS in propene conversion (X_P) followed by a plateau (Fig. 4a). However, for the lowest value of τ (0.0048 h), an initial increase of X_P can be observed. The change with TOS of the corrected conversion of toluene $(X_T)_C$ (taken as the ratio between the measured and the maximum values of toluene conversion obtained in the case of a totally selective monoisopropylation) is shown in Fig. 4b. Curiously, regardless of τ, there was an initial increase in $(X_T)_C$ followed by a plateau for TOS $\geqslant$ 45 min. An explanation of this induction period is proposed in Section 3.2.2.

3.2.1. Reaction products

The reaction products can be classified into six categories:

1. The desired products, that is, cymenes (*o*-, *m*-, and *p*-isomers), resulting from the isopropylation of toluene by propene.

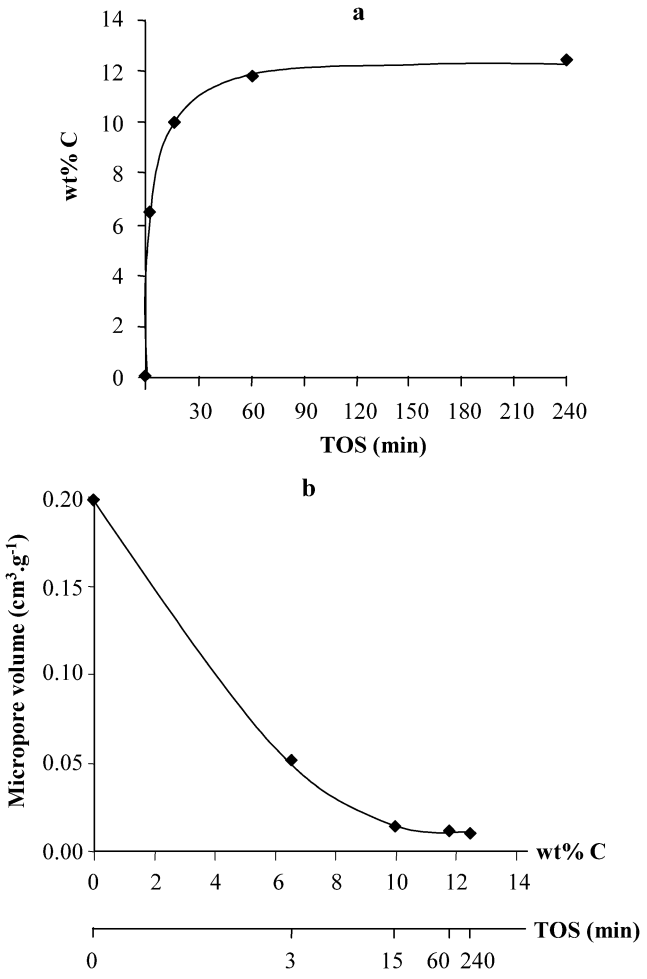

Fig. 5. Influence of time-on-stream (TOS) on coke formation (wt% C) (a) and effect of coke and TOS on the micropore volume accessible to nitrogen adsorbate (b).

2. C_{13} and C_{16} hydrocarbons produced by dialkylation and trialkylation of toluene with propene.
3. Benzene and xylenes produced by toluene disproportionation.
4. C_4–C_6 hydrocarbons (mostly alkenes) resulting from oligomerization cracking of propene.
5. C_{10} (other than cymenes), C_{11}, and C_{12} hydrocarbons with one aromatic ring. (C_{10}, formed in very low amounts, are composed of *n*-propyltoluenes, which are known to result from transalkylation between cymenes and toluene [20]; C_{11} and C_{12} result mainly from alkylation of toluene with butenes and pentenes; a very small part of the C_{11} and C_{12} hydrocarbons can also result from alkylation of xylenes by propene and butenes.)
6. Nondesorbed products (i.e., coke).

Regardless of the τ and TOS, only small amounts of 3 and 5 products were formed.

Fig. 5 shows that for $\tau = 0.0288$ h, there was a rapid deposition of coke followed by a plateau; this "coke" caused a significant blockage of the access of nitrogen adsorbate and hence of the reactant molecules to the micropores; V_{tp} is divided by 4 and 15 for deposits of 6.4 and 9.9 wt% C, respectively. This significant effect of coke on micropore volume indicates that coke was essentially formed and deposited within the inner micropores (supercages and sinusoidal channels) of the MCM-22 zeolite. However, the percentage of transformation of the propene–toluene mixture into coke was not very high; thus, even during the first 3 min of reaction, the deposit of coke corresponded to <3 wt% of the feed.

3.2.2. *Effect of TOS on the yield in the products*

The product distribution and the yields in the products formed for $\tau = 0.0288$ h and TOS = 2 and 240 min are given as an example in Table 2. On the fresh zeolite, 1 and 4 products were largely predominant, whereas at longer TOS, 1 and 2 (essentially C_{13}) were the main products.

The conversion of propene, X_P, was always greater than the corrected value of toluene conversion, $(X_T)_C$ (the ratio between the measured and the maximum values of toluene conversion by monoisopropylation). This indicates that the consumption of propene for forming secondary products (other than the desired cymenes), polyalkylated toluenes formed within the supercages and trapped because of their narrow apertures (hence considered coke) and C_4–C_6 was more significant than that of toluene. However, the difference between X_P and $(X_T)_C$, which was very significant at TOS = 2 min, became weak for TOS $\geqslant$ 45 min (Figs. 6a and b). This observation can be related to the significant decrease in the C_4–C_6 yield from propene (Fig. 7a), most likely due to the deposition of coke. The yields in the benzene–xylene products of toluene disproportionation (B + X), which were formed in low amounts, also decreased with increasing TOS (Fig. 7b). This decrease and that in the C_4–C_6 yield suggest that carbonaceous compounds (coke) are deposited in the pore systems in which both the oligomerization cracking of propene and the disproportionation of toluene occur.

Curiously, the yields in both the desired alkylation products [cymenes (Fig. 7c)] and the nondesired ones [C_{13} and C_{16} (Fig. 7d)] increased with increasing TOS. This induction period was similar to that observed in ethylbenzene disproportionation over large-pore zeolites [21] and over H-MCM-22 [22] and can be explained by the buildup of polyalkylated products. The buildup of polyalkylated toluene within the supercages of MCM-22 can explain part of the induction period observed in our experiments; an additional explanation would be the greater availability of propene for alkylation reactions because of the lower transformation of this reactant into C_4–C_6 and carbonaceous products.

3.2.3. *Reaction scheme*

The yields in the main products are plotted in Fig. 7 as a function of the contact time τ. The slopes of the tangent to all of the curves at $\tau = 0$ were positive, meaning that all of the reaction products were formed directly (these are apparent primary products). They resulted from the transformation either of only one reactant (e.g., C_4–C_6) from propene, benzene plus xylenes from toluene, or of both reactants (cymenes and C_{13} and C_{16}). This direct formation could be expected for all

Table 2
Transformation of a 2/1 toluene–propene mixture on the MCM-22 zeolite at 200 °C for a contact time $\tau = 0.0288$ h. Effect of time-on-stream (TOS)

	Distribution (wt%)			Yields (%) with respect to toluene/T or $C_3^=$/P		
TOS (min)	2	240		2	240	2–240
$C_3^=$	2.24	4.12	–	–	–	
C_4–C_6	3.79	0.29	/P	23.56	1.57	+21.99
Benzene	0.13	0	/T	0.18	0.	+0.15
Toluene	63.59	54.91	–	–	–	
Xylene	0.31	0.1	/T	0.32	0.1	+0.25
Cymenes	24.62	36.17	/T	20.2	30.22	−10.02
			/P	47.95	63.58	−15.63
C_{10}–C_{12}	1.23	0.16	/T	0.91	0.12	+0.79
C_{13}	3.68	4.20	/T	2.3	2.67	−0.37
C_{16}	0.41	0.07	/T	0.2	0.03	+0.17
Conversion						
X_P	86.1	76.86				
$(X_T)_C$	48.35	66.3				

X_P, propene conversion; $(X_T)_C$, corrected value of toluene conversion (see text).

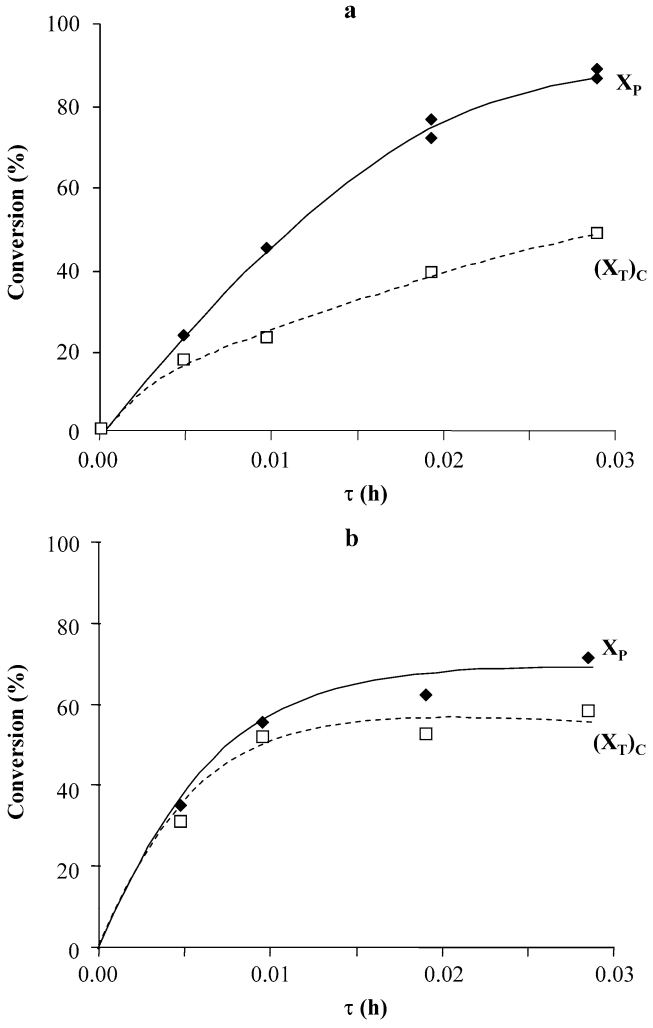

Fig. 6. Transformation of a 2/1 toluene–propene mixture over fresh [TOS = 2 min (a)] and stabilized [TOS = 45 min (b)] MCM-22 samples. Conversion of propene (X_P) and toluene ($(X_T)_C$) as a function of contact time τ.

of the products except C_{13} and C_{16}, which result from successive alkylation steps [reaction (1)]. This apparent direct formation and in a ratio practically independent on conversion and TOS (e.g., C_{13}/cymene molar ratio of 12–15) can be related to the activation of the aromatic ring by the isopropyl group, which makes the second alkylation step faster than the first step ($k_2 > k_1$)

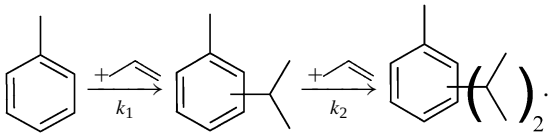

(1)

However, above two and especially three isopropyl groups, the alkylation becomes sterically limited, because of steric constraints in the zeolite pores and also between the isopropyl substituents in the aromatic ring.

The electrophilic isopropylation of toluene should lead preferentially to *ortho*- and *para*-isomers. Fig. 8 shows that this was the case at low conversion; at 10% conversion, the composition of the cymene mixture was 33% *para*, 37% *ortho*, and 30% *meta*, compared with 28.3% *para*, 14.7% *ortho*, and 57% *meta* at their thermodynamic equilibrium [23]. Unexpectedly, whereas steric constraints between methyl and isopropyl groups should limit formation of the *ortho* isomer, in fact this isomer was preferentially produced. This preferential formation of the *ortho* isomer, found for all the *ortho*-dialkylbenzenes [24], seems to be particular to the MCM-22 zeolite. Furthermore, as would be expected from a secondary reaction of isomerization, there was a significant increase with toluene conversion in the *m*-cymene percentage, essentially at the expense of *o*-cymene; the percentage of *p*-cymene, which at low conversion is close to the thermodynamic value, remained practically constant. Moreover, Fig. 8 indicates that cymene distribution did not depend on TOS and hence also not on the degree of zeolite deactivation.

The main reactions involved in the transformation of the propene–toluene mixture are reported in Scheme 1.

Experiments with pure toluene or pure propene were carried out to specify the effect of the second reactant on the reactions involving toluene only (i.e., disproportionation into benzene and xylenes) or propene only (i.e., oligomerization cracking). Propene had only a small effect on toluene disproportionation on fresh MCM-22, with an increase in the initial

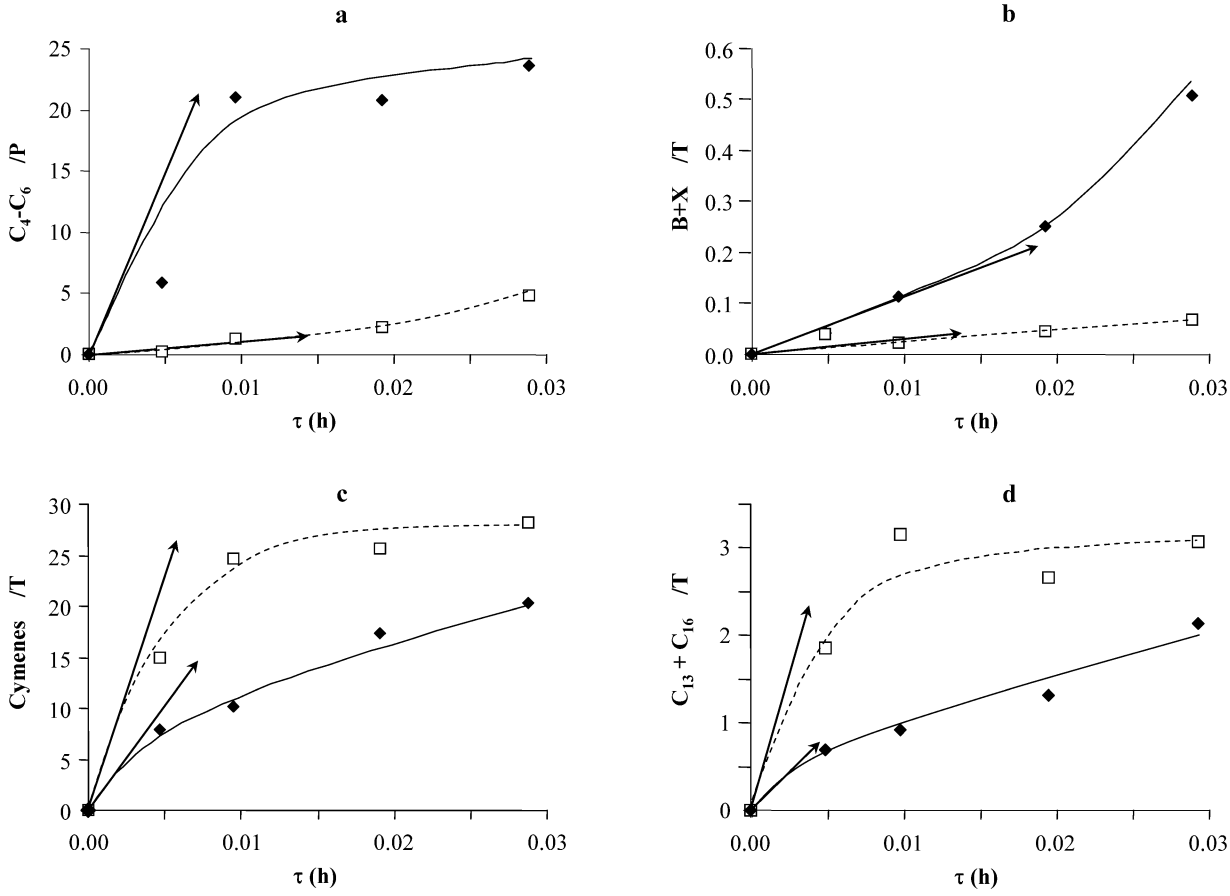

Fig. 7. Transformation of a 2/1 toluene–propene mixture over fresh (2 min reaction, plain line) and stabilized (45 min reaction, doted line) MCM-22 sample. Yields in the various products as a function of contact time τ.

production of benzene and especially of xylenes, but faster deactivation. In contrast, the effect of toluene on propene transformation through oligomerization cracking over fresh MCM-22 was very pronounced, with production of C_4–C_6 in the presence of toluene and also of C_7 and even C_8 in its absence, along with a significant decrease in the yield of aliphatic products (e.g., for TOS = 1 min, 85% from pure propene to 33% from the propene–toluene mixture). This decrease can be ascribed to the trapping by toluene of isopropylcarbenium ions resulting from propene adsorption over protonic sites with cymene production, along with the competition between toluene and propene for adsorption on the protonic sites, resulting in a decrease in the concentration of isopropylcarbenium ions and hence also in the rate of oligomerization-cracking reactions. Furthermore, toluene had practically no effect on the deactivation associated with the oligomerization-cracking process.

3.3. Location of the reactions

Information on the location of the various reactions can be drawn from the effect of TOS (and hence of coke) on their rate. An important remark is that although there was, at least for $\tau = 0.0288$ h, a quasicomplete blockage of the access to the micropores for TOS $\geqslant$ 15 min (Fig. 5), high values of X_P and $(X_T)_C$ can be observed. This indicates that at the plateau of conversion, the reactant transformation occurred essentially on the protonic sites of the external cups and with practically no deactivation, and that on fresh zeolite the transformations occurred not only within the external cups, but also within the inner micropores, with formation of desorbed products and nondesorbed products (i.e., coke).

3.3.1. Reactions within the external cups

Furthermore, because coke formation within the external cups is unlikely (no possible trapping of molecules), deactivation of the protonic sites located in these cups can be neglected. Therefore, the significance of the reactions occurring on these sites could be established by extrapolating the product distribution and yields at long TOS. Two main types of products can be observed for high TOS values: cymenes and C_4–C_6 alkenes. Whereas a plateau in the yield of cymenes with respect to toluene was found for TOS $\geqslant$ 30 min ($\sim$30% for $\tau = 0.0288$ h) (Fig. 9c), the yield in C_4–C_6 alkenes with respect to propene decreased rapidly (from 20–33% to 8% with an increase in TOS from 1 to 15 min), then more slowly: from 8% at 15 min to 2.2% at 60 min, 1.3% at 120 min, and 0.6% at 240 min (Fig. 9d). This continuous decrease suggests that most likely this reaction could disappear completely at very long TOS. Whatever the reason, toluene alkylation occurred within the external cups with a very high selectivity. Furthermore, even at long TOS, a very slow and stable production of xylene (yield with respect to toluene of 0.1%) can be observed, curiously without

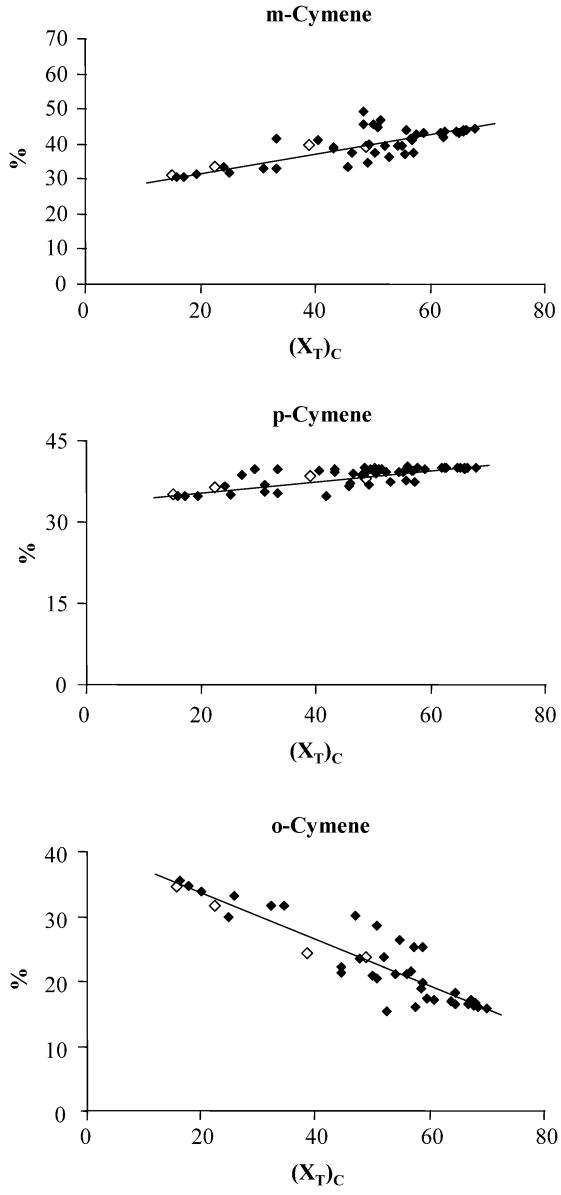

Fig. 8. Transformation of a 2/1 toluene–propene mixture at 200 °C on MCM-22 zeolite. Distribution of cymene isomers as a function of toluene conversion $(X_T)_C$. Empty symbols, time on stream (TOS) of 2 min; filled symbols, other TOS values.

the corresponding formation of benzene expected from toluene disproportionation (Table 2).

The role of the protonic acid sites of the external cups in the production of alkylates (mono- and diisopropyltoluenes) can be confirmed by poisoning selectively these sites by a bulky basic molecule. 2,4-DMQ, which was previously shown [6] to selectively poison the acidic sites of the external surface cups active in *m*-xylene transformation at 350 °C, is not sufficiently volatile ($bp_{760} = 265$ °C) for use as a poison in the low-temperature toluene alkylation. Thus we substituted a more volatile bulky basic molecule, γ-collidine ($bp_{760} = 171$ °C), which cannot enter the inner micropores of MCM-22 or cause any limitation in access to the inner acidic sites [25].

Fig. 9 shows the effect of the presence of collidine (18.6 µmol min^{-1} $g^{-1}_{zeolite}$) on the conversion of the reactants X_P and $(X_T)_C$

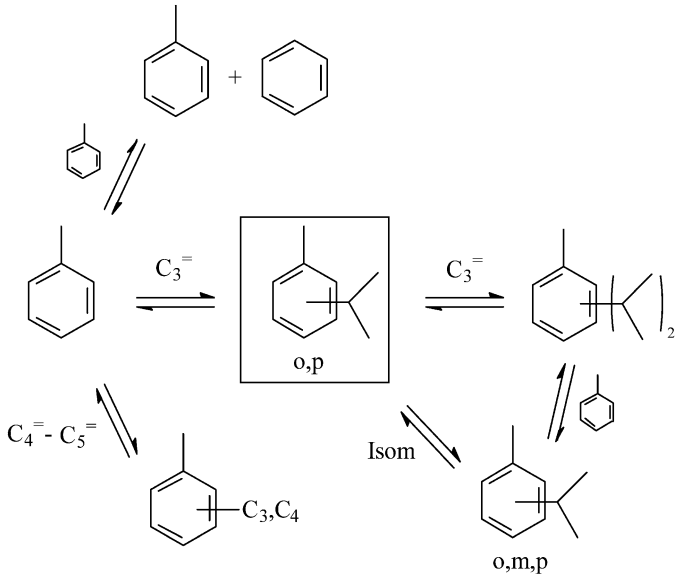

Scheme 1. Transformation of a toluene–propene mixture over MCM-22 zeolite. Reaction scheme.

(Figs. 9a and b) as well as on the yields in the main products, cymenes (Fig. 9c) and C_4–C_6 alkenes (Fig. 9d). Collidine caused a significant decrease in both propene and toluene conversion (Figs. 9a and b), as well as in cymene (Fig. 9c) and other alkylate (C_{13}, C_{16}) production. The ratio between diisopropyltoluenes and cymenes was not affected by poisoning. In contrast, poisoning with collidine caused a change in cymene distribution, with an increase in the percentage of *o*-cymene at the expense of *m*-cymene. This means that collidine caused not only a poisoning of cymene production, but also a more pronounced poisoning of the subsequent isomerization.

The effect of collidine was more complicated on C_4–C_6 production than on alkylate production, with an initial increase followed by a decrease. After 20–30 min (i.e., after injection of 370–560 µmol of collidine $g^{-1}_{zeolite}$), no reaction products can be observed. This means that all of the reactions were suppressed because of poisoning with collidine or deactivation by coking. The quasitotal suppression of C_4–C_6 products suggests that a very small part of these products (1.6% for $\tau = 0.0288$ h; i.e., 40 times less than cymenes) could be formed in the external cups. Furthermore, the initial increase in C_4–C_6 production caused by collidine poisoning can be explained by the poisoning of toluene alkylation; the propene molecules that do not participate in alkylation can be transformed through the oligomerization-cracking process.

To show quantitatively the effect of collidine on the production of cymenes, the difference in yields in absence and in presence of collidine was determined and plotted as a function of TOS (Fig. 10). The amount of poison molecules passing through the catalyst bed (Q) is also indicated in abscissa. By supposing that at short TOS values, all of the collidine molecules have a poisoning effect, the values of TOS and Q used to obtain the maximum deactivation are given by point A in Fig. 10. The Q value of 80–90 µmol g^{-1} of zeolite was

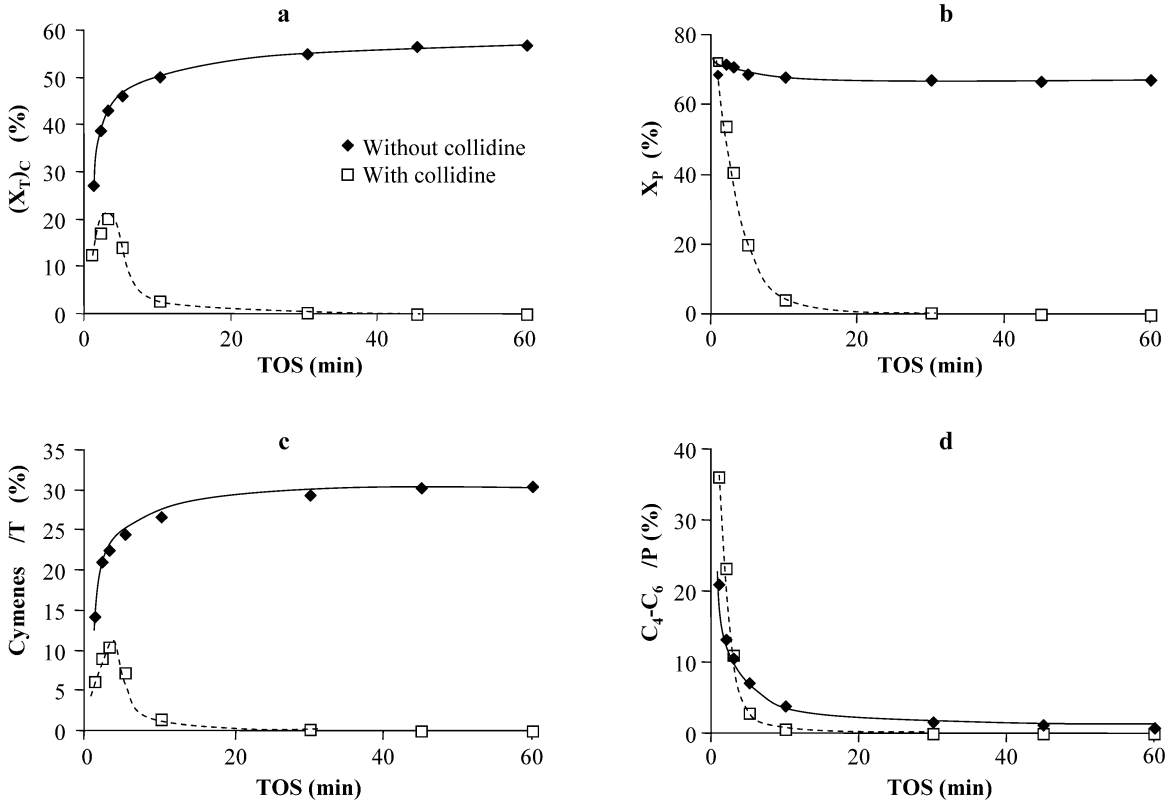

Fig. 9. Transformation of a 2/1 toluene–propene mixture over a H-MCM-22 zeolite. Effect of collidine poisoning. Conversion of toluene $(X_T)_C$ (a), of propene X_P (b) and yields in cymenes (c) and C_4–C_6 hydrocarbons (d) as a function of time-on-stream (TOS).

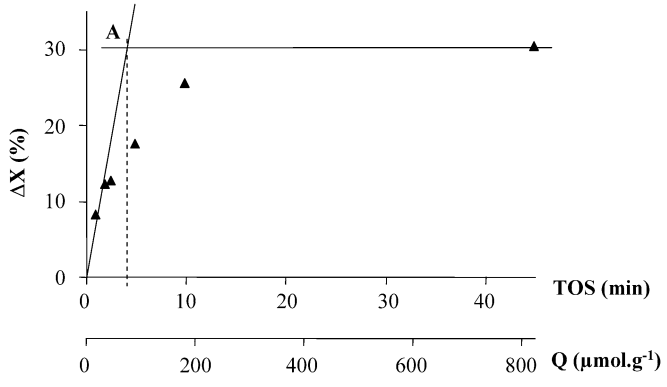

Fig. 10. Decrease in cymene yield (ΔX) as a function of time-on-stream (TOS) and of the amount of collidine added (Q) during the gas phase transformation of a 2/1 toluene–propene mixture at 200 °C over a H-MCM-22 zeolite.

very close to the concentration of protonic sites in the external cups estimated by 2,4-DMQ adsorption and to that of sites active in *m*-xylene transformation estimated by 2,4-DMQ poisoning.

The average activity in cymene production of each protonic site in the external hemicages (i.e., the turnover frequency [TOF]) was estimated by dividing the activities of the zeolite catalyst by the concentration of active protonic sites. The activity of the zeolite catalyst for cymene production drawn from Fig. 7c (i.e., slope of the initial tangent to the curve for TOS = 45 min) was found to be equal to 360 mmol h^{-1} g^{-1}, with a TOF of 4200 h^{-1}.

3.3.2. *Reactions within the inner micropores*

The yields in the products formed on the protonic sites of the inner micropores can be estimated by simple difference between the yields measured at very short and very long TOS values. Table 2 shows that the sites of the inner micropores were the active sites for the formation of C_4–C_6 alkenes through oligomerization cracking of propene (yield of ∼15% with respect to propene for $\tau = 0.0288$ h) and for the slow toluene disproportionation (yield of 0.4%). Most likely, this latter reaction, which involves bulky methyldiphenylmethane intermediate, could not occur in the narrow sinusoidal channels and hence would be catalyzed by the protonic sites of the large supercages only. The positive effect of propene on the initial rate of toluene disproportionation and the initial molar xylene/benzene ratio much higher than 1 suggest a complex reaction scheme. These products (and also part of the C_4–C_6 alkenes) could result from many successive reactions in a "hydrocarbon pool" trapped within the large supercages because of their small apertures. This idea was previously advanced to explain the distribution of the products of *m*-xylene transformation within the MCM-22 supercages [8]. However, part of the C_4–C_6 products could also be formed within the narrow sinusoidal channels through a simple oligomerization cracking of propene. Indeed, this latter reaction involves only nonbulky molecules and carbenium ions as intermediates, and these can be easily accommodated within the sinusoidal channel pore system. In this case, deactivation of the oligomerization-cracking process could be due to the formation and the trapping in the sinusoidal channels of molecules

too bulky to desorb from the sinusoidal channels and very stable because of their nature or their location far from the acidic sites. Indeed, even after treatment of the deactivated MCM-22 sample for 1 h under nitrogen flow at the reaction temperature, no increase in the production of C_4–C_6 alkenes can be observed.

To estimate the participation of the protonic sites in the production of C_4–C_6 alkenes within the sinusoidal channels, the transformation of the toluene–propene mixture was investigated over a MCM-22 sample deactivated for 24 h during *m*-xylene transformation at 350 °C. Indeed we previously showed that with this zeolite, all of the active sites of the supercages were deactivated by coke deposits [8]. Therefore, the C_4–C_6 alkenes observed should be produced within the sinusoidal channels.

Only small differences (in the range of experimental error) can be observed between the yields in C_4–C_6 alkenes on fresh and *m*-xylene-deactivated MCM-22 samples, suggesting that C_4–C_6 alkenes were formed mainly within the sinusoidal channels. Furthermore, quasiidentical yields in cymenes were obtained on the fresh and aged samples, confirming that alkylation of toluene with propene occurred essentially within the external cups.

In agreement with this proposal of oligomerization cracking of propene within the sinusoidal channels, C_4–C_6 products can be observed in larger amounts (1.7 times greater) in the presence of *o*-xylene, which cannot easily enter the sinusoidal channels [7], than in the presence of toluene. Moreover, C_7 and C_8 were also produced from pure propene, whereas these compounds were not formed from the toluene–propene mixture.

4. Conclusions

From this study of the transformation of a 2/1 molar toluene–propene mixture over a MCM-22 sample, the following conclusions can be drawn:

1. Over the fresh catalyst, oligomerization cracking of propene with C_4–C_6 production and toluene alkylation into cymenes and diisopropyltoluenes are the main reactions. The formation of carbonaceous deposits causes the progressive suppression of the oligomerization-cracking reactions without affecting the formation of alkylates.
2. Nitrogen adsorption demonstrates that the suppression of C_4–C_6 production comes from the blockage of the access to the inner micropores. The continuous alkylation of toluene occurs essentially on the protonic sites of the external cups and this with no detectable deactivation.
3. Poisoning by collidine confirms that toluene alkylation occurs essentially on the protonic sites of the external cups. It can be therefore considered that after aging, H-MCM-22 samples with large external surface or even better delaminated ITQ-2 zeolites will be very active, stable, and selective catalysts for the alkylation of aromatics with propene.
4. Comparing the transformation of the toluene–propene mixture over fresh and over *m*-xylene-deactivated MCM-22 samples suggests that oligomerization cracking of propene occurs mainly within the sinusoidal channels.

References

[1] M.K. Rubin, P. Chen, US patent 4,954,325 (1990), assigned to Mobil Oil Corp.
[2] J.S. Beck, A.B. Dandekar, T.F. Degnan, in: M. Guisnet, J.P. Gilson (Eds.), Zeolites for Cleaner Technologies, Catalytic Science Series, vol. 3, Imperial College Press, London, 2002, p. 223.
[3] C. Perego, P. Ingallina, Catal. Today 73 (2002) 3.
[4] M.E. Leonowicz, S.L. Lawton, R.D. Partridge, P. Chen, M.K. Rubin, Science 264 (1994) 1910.
[5] S.L. Lawton, M.E. Leonowicz, R.D. Partridge, P. Chen, M.K. Rubin, Microporous Mesoporous Mater. 23 (1998) 109.
[6] S. Laforge, D. Martin, M. Guisnet, Microporous Mesoporous Mater. 67 (2004) 235.
[7] S. Laforge, D. Martin, M. Guisnet, Appl. Catal. A 268 (2004) 33.
[8] S. Laforge, D. Martin, J.-L. Paillaud, M. Guisnet, J. Catal. 220 (2003) 92.
[9] C. Perego, S. Amarilli, R. Millini, G. Bellussi, G. Girotti, G. Terzoni, Microporous Mater. 6 (1996) 395.
[10] A. Corma, V. Martinez-Soria, E. Schnoeveld, J. Catal. 192 (2000) 163.
[11] J. Cejka, A. Krejci, N. Zilkova, J. Kotrla, S. Ernst, A. Weber, Microporous Mesoporous Mater. 53 (2002) 121.
[12] J.C. Cheng, T.F. Degnan, J.S. Beck, Y.Y. Huang, M. Kalyanaraman, J.A. Kowalski, C.A. Loehr, D.N. Mazzone, Stud. Surf. Sci. Catal. 121 (1999) 53.
[13] A. Corma, C. Corell, J. Perez-Pariente, Zeolites 15 (1995) 2.
[14] M. Guisnet, P. Ayrault, J. Datka, Polish J. Chem. 71 (1997) 1455.
[15] P. Ayrault, J. Datka, S. Laforge, D. Martin, M. Guisnet, J. Phys. Chem. B 108 (2004) 13755.
[16] W.D. Harkins, G. Jura, J. Chem. Phys. 11 (1943) 431.
[17] D. Meloni, S. Laforge, D. Martin, M. Guisnet, E. Rombi, V. Solinas, Appl. Catal. A 215 (2001) 55.
[18] A. Corma, C. Corell, V. Fornés, W. Kolodziejski, J. Perez-Pariente, Zeolites 15 (1995) 576.
[19] B. Onida, F. Geobaldo, F. Testa, F. Crea, E. Garrone, Microporous Mesoporous Mater. 30 (1999) 119.
[20] B. Wichterlova, J. Cejka, J. Catal. 146 (1994) 523.
[21] V. Weiss, M. Weihe, M. Hunger, H.G. Karge, J. Weitkamp, Stud. Surf. Sci. Catal. 105 (1997) 973.
[22] H.G. Karge, S. Ernst, M. Weihe, V. Weiss, J. Weitkamp, Stud. Surf. Sci. Catal. 84 (1994) 1805.
[23] Calculated using the Outokumpu HSC 5.1 for Windows software.
[24] T.F. Degnan Jr., J. Catal. 216 (2003) 32.
[25] H. Du, D.H. Olson, J. Phys. Chem. B 106 (2002) 395.